

CoMMA: Contribution-Aware Medical Multi-Agents From A Game-Theoretic Perspective

Yichen Wu ^{*1} Yujin Oh ^{*1} Sangjoon Park ^{*23} Kailong Fan ¹ Dania Daye ⁴ Hana Farzaneh ⁴ Xiang Li ⁴
Raul Uppot ⁴ Quanzheng Li ¹

Abstract

Recent multi-agent frameworks have broadened the ability to tackle oncology decision support tasks that require reasoning over dynamic, heterogeneous patient data. We propose Contribution-Aware Medical Multi-Agents (CoMMA), a decentralized LLM-agent framework in which specialists operate on partitioned evidence and coordinate through a game-theoretic objective for robust decision-making. In contrast to most agent architectures relying on stochastic narrative-based reasoning, CoMMA utilizes deterministic embedding projections to approximate contribution-aware credit assignment. This yields explicit evidence attribution by estimating each agent's marginal utility, producing interpretable and mathematically grounded decision pathways with improved stability. Evaluated on diverse oncology benchmarks, including a real-world multidisciplinary tumor board dataset, CoMMA achieves higher accuracy and more stable performance than data-centralized and role-based multi-agents baselines. Source code will be released upon publication.

1. Introduction

Effective clinical decision support in oncology, such as treatment recommendation, prognosis estimation, and recurrence prediction, requires the seamless integration of longitudinal, heterogeneous data. In practice, this process is carried out through multidisciplinary tumor boards (Taylor et al.,

2010; Patkar et al., 2011), where clinicians jointly discuss patient histories, medical imaging, pathology findings, and evolving laboratory markers. Replicating the collaborative reasoning process remains challenging for AI systems, as it demands robust reasoning over high-dimensional, dynamically structured evidence with clear attribution. Recently, large language model (LLM)-based multi-agents systems have emerged as a promising paradigm for this setting, distributing complex multimodal reasoning across specialized agents to better reflect multidisciplinary clinical decision-making (Chen et al., 2025b; Kim et al., 2024; Ferber et al., 2025; Han et al., 2025; Fallahpour et al., 2025).

Despite their promise, most medical multi-agent frameworks implement collaboration through role-play, assigning clinician-like personas such as oncologists or radiologists (Chen et al., 2025b; Kim et al., 2024; Zhang et al., 2025). This setup often relies on long-form dialogue as the coordination channel, which increases interaction overhead and makes outcomes sensitive to conversational dynamics. More importantly, these systems are typically data-centralized, exposing all agents to the same full patient context. In this case, role specialization is largely semantic rather than structural, and it becomes difficult to isolate which evidence drives a decision or to assign responsibility when errors occur. As a result, current frameworks offer limited clinician-facing explainability and incur high inference cost, as shown in Figure 1(a) and (b).

To address these limitations, we propose Contribution-Aware Medical Multi-Agents (CoMMA), a framework that replaces role-based interaction with data-decentralized specialization. As illustrated in Figure 1(c), CoMMA partitions the clinical context into distinct information streams and assigns each to a dedicated agent, enforcing specialization by construction rather than by persona simulation. Agent communication is conducted through deterministic embedding projections instead of natural language dialogue, and the final clinical decision is formed by aggregating agent outputs with learnable contribution weights. This design improves scalability, reduces inference cost, and preserves clinical data privacy compared to data-centralized and role-based multi-agent systems, as summarized in Table 1.

^{*}Equal contribution ¹Center for Advanced Medical Computing and Analysis (CAMCA), Department of Radiology, Massachusetts General Hospital and Harvard Medical School, MA 02114, USA ²Department of Radiation Oncology, Yonsei University College of Medicine, Yonsei University, Seoul 03772, Republic of Korea ³Institute for Innovation in Digital Healthcare, Yonsei University, Seoul 03772, Republic of Korea ⁴Interventional Radiology Academic Medical Centers, Mass General Brigham, MA 02114, USA. Correspondence to: Quanzheng Li <Li.Quanzheng@mgh.harvard.edu>, Raul Uppot <ruppot@mgb.org>.

Table 1. Comparison on agent AI frameworks for oncology decision-making.

	(a) Single-Agent	(b) Role-based Multi-Agents	(c) Contribution-Aware Multi-Agents (Ours)
Data Stream	Centralized global view	Centralized-distributed	Decentralized specialized view
Evidence Contribution Attribution	Implicit	Role assignment	Explicit, Game-theoretic contribution modeling
LLM Functional Role	Generative modeling	Generative modeling	Deterministic embedding projection
Output Format	Narrative (> 1,500 chars)	Narrative (> 10,000 chars)	Class-wise logits
Inference	Online (\$ / token)	Online (\$ / token)	Offline (local GPU required)
Clinical Privacy Architecture	Cloud-based inference		Strictly local inference

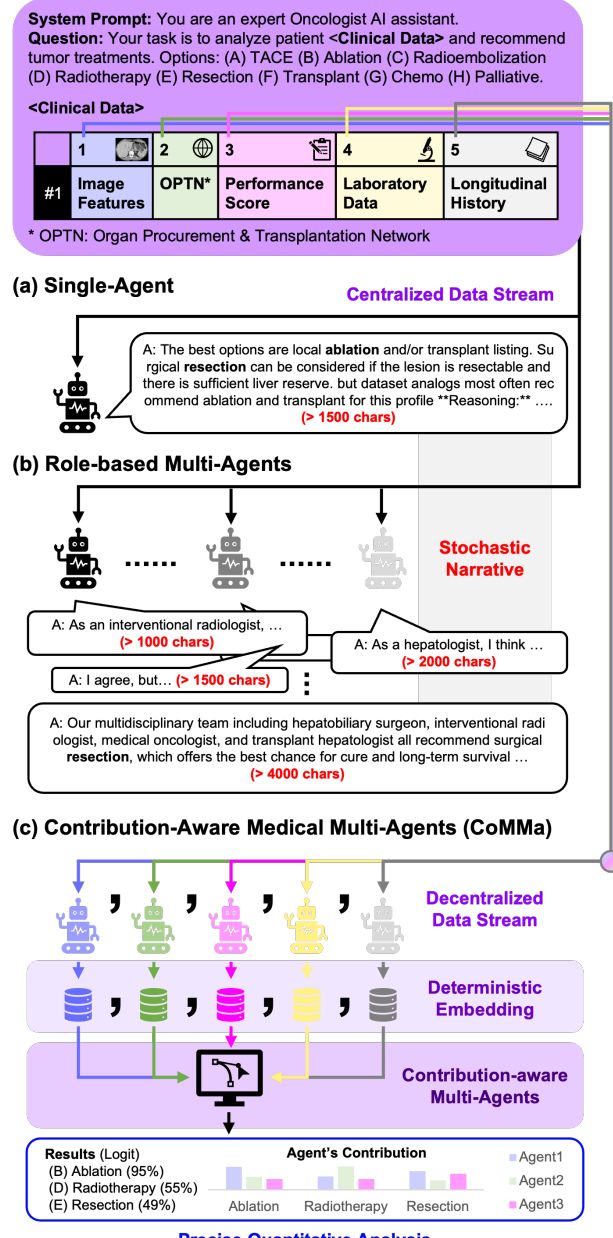


Figure 1. (a) Single-agent and (b) Role-based frameworks rely on stochastic narratives, which are often costly and difficult to audit. In contrast, (c) CoMMA leverages data-decentralized agent specialization and deterministic embeddings to facilitate contribution-aware optimization and precise quantitative analysis.

Moreover, our CoMMA is grounded in cooperative game theory, where clinical decision-making is modeled as a coalitional process among agents. We adopt the principle of Shapley value (Shapley, 1953; Beechey et al., 2023) to regularize contribution learning, aligning each agent’s learned contribution weight with its estimated marginal utility. By minimizing the Kullback–Leibler (KL) divergence between these quantities, CoMMA enables explicit and stable credit assignment, transforming multi-agent collaboration from a stochastic dialogue process into a structured and interpretable inference procedure. This contribution-aware formulation directly addresses the stability requirements of clinical decision support.

To verify the effectiveness of our CoMMA, we evaluate it across a diverse set of oncology benchmarks, with a real-world multidisciplinary tumor board dataset as a key testbed. Experimental results demonstrate that CoMMA achieves state-of-the-art performance with significantly higher decision stability over data-centralized baselines.

Our core contributions are summarized as follows:

- We transition from stochastic text-based agent communication to a deterministic embedding framework, enabling a stable, locally fine-tunable architecture suitable for clinical deployment.
- We introduce a multi-agent modeling approach that ensures precise credit assignment across decentralized data streams, offering a transparent mechanism to evaluate the influence of specific data modalities.
- We demonstrate that CoMMA outperforms existing frameworks in predictive accuracy and interpretability across complex, multidisciplinary oncology scenarios, establishing a new state-of-the-art for agentic clinical decision support.

2. Related Works

2.1. Multi-Agents for Medical Applications

Recent studies have explored multi-agent LLM systems for collaborative clinical decision-making, where agents take specialized medical roles (Chen et al., 2025a; Tang et al., 2025; Zou & Topol, 2025; Johri et al., 2025; Wang et al., 2025; Zhou et al., 2025; Almansoori et al., 2025;

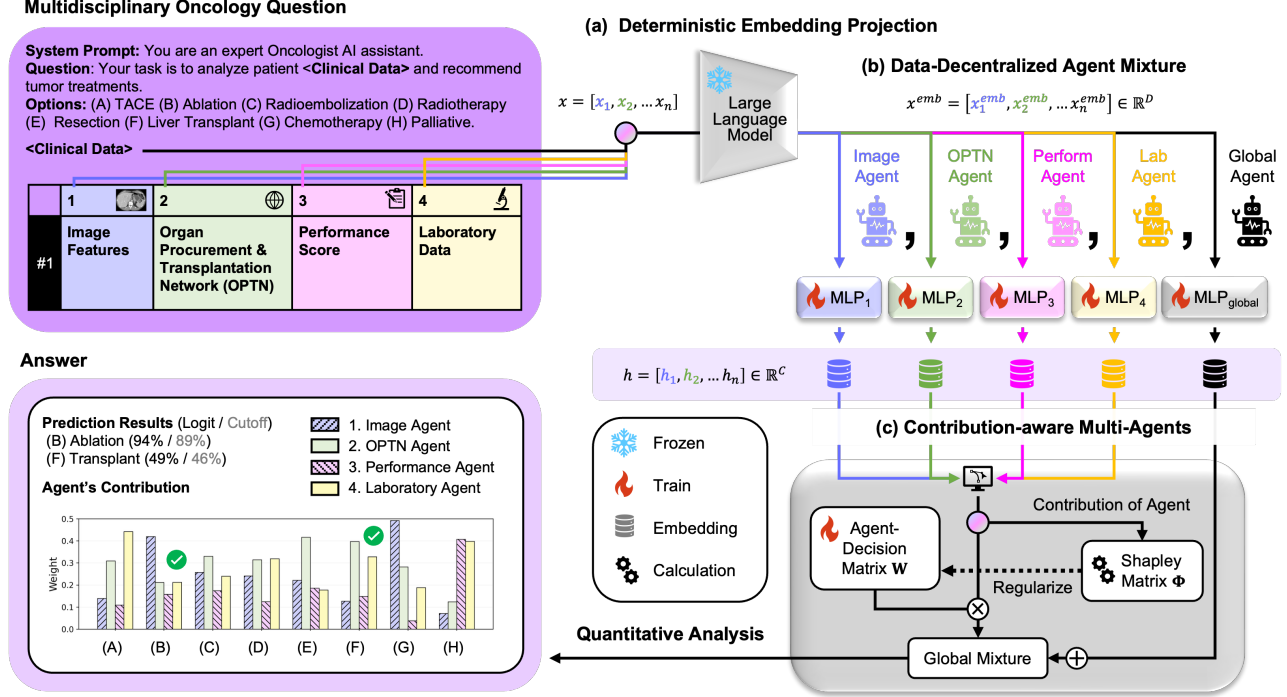


Figure 2. Architectural workflow of the CoMMA framework for multi-agent oncology decision support. (a) Deterministic embedding projection module encodes text inputs into a shared embedding space using a frozen LLM. (b) Data-decentralized agent mixture module routes each embedding to its designated partition agent and processes it via a learnable MLP. (c) Contribution-aware multi-agent module aggregate agent-specific representations using an agent-decision matrix, which is regularized by a Shapley-based contribution matrix. In the answer, we quantitatively assess each agent’s contribution. Class-wise logits and decision cutoffs are transformed into percentiles.

Fallahpour et al., 2025). MedAgents (Tang et al., 2024) frames problem-solving as a multi-physician debate with answer aggregation, while MDAgents (Kim et al., 2024) adaptively chooses single-versus multi-agent collaboration to balance accuracy and cost. Beyond free-form discussion, Multi-Agent Conversation (Chen et al., 2025b) structures deliberation to mimic multidisciplinary meetings, and AI Hospital (Fan et al., 2025) evaluates longitudinal reasoning in a multi-agent clinical simulation. However, these systems are primarily role-based: collaboration is mediated through narrative exchanges and the final decision is fused implicitly, making evidence-level contribution hard to quantify. In contrast, our contribution-aware framework explicitly attributes how each evidence source and agent influences the final prediction, enabling more controlled fusion and more reliable clinical decision outputs.

2.2. Game Theory in Clinical Decision-Making

Game theory provides mathematical frameworks for modeling strategic interactions among rational agents and has been widely applied in general-domain decision-making, including economics, management, defense, and computer science (Von Neumann & Morgenstern, 2007; Dutang et al., 2013; Ho et al., 2022; Parsons & Wooldridge, 2002; Lanctot et al.,

2017). Despite its strong theoretical foundations, its adoption in clinical settings remains limited (Mendonça et al., 2020; Lau et al., 2023), particularly in oncology. Oncology decision-making relies on heterogeneous and interdependent evidence sources, where quantifying the contribution of each component is essential for interpretability and clinical reliability. Among cooperative game-theoretic approaches, the Shapley value (Shapley, 1953; Beechey et al., 2023) provides a principled and axiomatized solution for fair allocation of a total payoff among participating agents. In a clinical AI setting, the payoff corresponds to the final clinical decision or predictive outcome, while each agent represents a distinct modality or specialized source of clinical information. The Shapley value of an agent is defined as its expected marginal contribution, averaged over all possible coalitions, satisfying desirable payoff. To the best of our knowledge, this work is the first to incorporate Shapley value-based contribution modeling as a regularization mechanism in a multi-agent oncological tumor board framework.

3. Method

In this section, we provide a detailed schematic of CoMMA, as illustrated in Figure 2. We first introduce the deterministic embedding projections in Section 3.1, followed by the

data-decentralized agent mixture in Section 3.2. Finally, in Section 3.3, we elaborate on the game-theoretic formulation that governs our contribution-aware multi-agent system.

3.1. Deterministic Embedding Projection

In clinical decision support, we consider the problem of predicting outcomes from heterogeneous, multimodal patient data $\mathbf{x} = \{\mathbf{x}_1, \mathbf{x}_2, \dots, \mathbf{x}_N\}$. Each text-based input \mathbf{x}_i distinct clinical information source, such as medical imaging reports, longitudinal laboratory measurements, or patient clinical history. To mitigate the stochasticity and hallucination-prone intermediate outputs of LLM, we introduce a deterministic projection operator F_θ that maps each clinical text partition to a latent representation. Formally, for a given textual input \mathbf{x}_i , the projection is defined as:

$$\begin{aligned} \mathbf{x}_i^{emb} &= \text{LLM}_{\text{frozen}}(\mathbf{x}_i)[\text{<CLS>}], \\ F_\theta(\mathbf{x}_i) &= \text{MLP}_\theta(\mathbf{x}_i^{emb}), \end{aligned} \quad (1)$$

where $\text{LLM}_{\text{frozen}}$ serves as the fixed encoder for the input \mathbf{x} , as detailed in Figure 2(a). To capture the salient clinical evidence without the overhead of full-sequence generation, we extract the hidden embedding of the terminal <CLS> (or | endoftext |) token embedding from the LLM’s final layer. This projected embedding $\mathbf{x}_i^{emb} \in \mathbb{R}^D$ functions as a D -dimensional bottleneck representation. The parameter θ the weights of a subsequent Multilayer Perceptron (MLP) projection that maps \mathbf{x}_i^{emb} into a task-specific latent space. This operator constitutes the fundamental building block of each agent within our decentralized framework.

3.2. Data-Decentralized Agent Mixture

In this subsection, we contrast two distinct modeling paradigms: a standard data-centralized approach and our proposed decentralized, contribution-aware approach.

Data-Centralized Formulation. In this paradigm, a single global operator F_θ observes the entire concatenated input at once, and multimodal clinical evidence is integrated implicitly through the model’s self-attention:

$$\hat{\mathbf{y}} = F_\theta([\mathbf{x}_1; \dots; \mathbf{x}_N]), \quad (2)$$

where $\hat{\mathbf{y}} \in \mathbb{R}^C$ is the predicted logit vector across C categories, $[\cdot; \cdot]$ denotes string concatenation, and the parameters θ are updated by minimizing the empirical risk $\mathcal{L}_{\text{BCE}}(\hat{\mathbf{y}}, \mathbf{y})$, where $\mathbf{y} \in \mathbb{R}^C$ is the ground truth label. While effective, this formulation provides no explicit mechanism to isolate the effect of each information stream, making evidence attribution and responsibility assignment inherently ambiguous.

Data-Decentralized Formulation. In CoMMA, as illustrated in Figure 2(b), each agent i applies the projection operator only to its designated partition \mathbf{x}_i , yielding a set of

specialized embeddings:

$$\mathbf{h}_i = f_{\theta_i}(\mathbf{x}_i), \quad (3)$$

where θ_i represents the learnable parameters of the i -th agent’s projection head and $\mathbf{h}_i \in \mathbb{R}^C$ is the agent’s logit vector over C categories. By isolating information streams at the input level, we can explicitly measure each agent’s utility before final aggregation. The final prediction is then produced through a two-stage weighted aggregation.

3.2.1. AGENT-WISE AGGREGATION.

The specialized embeddings $\{\mathbf{h}_1, \dots, \mathbf{h}_N\}$ are fused using a learnable agent-decision matrix $\mathbf{W} \in \mathbb{R}^{N \times C}$, where $W_{i,k}$ represents the contribution weight of agent i for output dimension k . The aggregated representation $\mathbf{z}_A \in \mathbb{R}^D$ is computed as:

$$z_{A,k} = \sum_{i=1}^N W_{i,k} \cdot h_{i,k}, \quad \text{for } k = 1, \dots, C. \quad (4)$$

We normalize \mathbf{W} so that $\sum_{i,k} W_{i,k} = 1$ making $W_{i,k}$ directly interpretable as a per-class contribution weight. This aggregation yields a structured mixture over agent predictions, enabling explicit credit assignment across agents.

3.2.2. GLOBAL MIXTURE.

Decentralized specialization extracts complementary evidence, but clinical decisions still require a unified patient-level summary. We therefore introduce a global mixture module that combines the aggregated representations \mathbf{z}_A with a global clinical anchor $\mathbf{x}_{\text{global}}$. The final prediction $\hat{\mathbf{y}} \in \mathbb{R}^C$ is given by,

$$\hat{\mathbf{y}} = \text{MLP}_\phi(\tilde{w}_A \cdot \mathbf{z}_A + \tilde{w}_G \cdot f_{\theta_{\text{global}}}(\mathbf{x}_{\text{global}})), \quad (5)$$

where MLP_ϕ denotes a task-specific projection head, and $\{\tilde{w}_A, \tilde{w}_G\}$ are learnable mixture weights. Here, we define $f_{\theta_{\text{global}}}$ as the global agent, which operates on the global anchor $\mathbf{x}_{\text{global}}$. This anchor is selected as the most comprehensive modality available within the dataset \mathbf{x} (e.g., the primary clinical history or the concatenated entire input sequence) to provide a unified reference. Additional details are provided in Section A.1. By synthesizing these streams, the mixture mechanism leverages heterogeneous, modality-specific features while ensuring they remain anchored to a global clinical grounding.

3.3. Contribution-aware Multi-Agents

To ensure the agent-decision matrix \mathbf{W} provides a faithful representation of clinical evidence, we reformulate the multi-agent collaboration as a cooperative coalitional game. In this setting, the predictive performance serves as the game’s

reward function, and we aim to align the learned weights W_i with the agents' respective Shapley values, which represent the only fair distribution of credit based on marginal utility. The final optimization step integrates the supervised classification signal with the agentic objectives defined as:

$$\mathcal{L}_{\text{total}} = \mathcal{L}_{\text{BCE}}(\hat{\mathbf{y}}, \mathbf{y}) + \lambda_{\text{pg}} \mathcal{L}_{\text{pg}} + \lambda_{\text{shap}} \mathcal{L}_{\text{shap}}, \quad (6)$$

where \mathcal{L}_{BCE} is the standard binary cross-entropy loss for multi-label classification, \mathcal{L}_{pg} is a policy-gradient term that updates \mathbf{W} using advantage signals to upweight agent-class pairs with positive marginal utility, and $\mathcal{L}_{\text{shap}}$ regularizes \mathbf{W} toward Shapley-based credit assignment. We defer the definitions of \mathcal{L}_{pg} and $\mathcal{L}_{\text{shap}}$ to the following subsections. In this setting, the model is prevented from collapsing into a state where a single agent disproportionately influences the output without demonstrably improving the objective.

3.3.1. AGENT-WISE REWARD AND ADVANTAGE

The first step in calculating these auxiliary objectives is to quantify the individual utility of each agent. The credit assignment mechanism utilizes agent-wise reward vectors $\mathbf{r}'_i \in \mathbb{R}^C$. The reward for agent i on dimension k is defined by the marginal reduction in $\mathcal{L}_k^{\text{BCE}}$ achieved by its inclusion:

$$r'_{i,k} = \mathcal{L}_k^{\text{BCE}}(\hat{\mathbf{y}}_{-i}, \mathbf{y}) - \mathcal{L}_k^{\text{BCE}}(\hat{\mathbf{y}}, \mathbf{y}), \quad (7)$$

where $\hat{\mathbf{y}}_{-i}$ is the prediction generated when excluding agent i from the coalition. To reduce variance in the gradient estimation, we define the advantage vector $\mathbf{A}_i = \mathbf{r}'_i - \mathbf{b}$, where $\mathbf{b} = \frac{1}{N} \sum_{j=1}^N \mathbf{r}'_j$ serves as the baseline.

3.3.2. POLICY-GRADIENT LOSS

Using the advantage vector \mathbf{A}_i derived above, we optimize the *agent-decision matrix* \mathbf{W} (introduced in Section 3.2.1). The policy-gradient term \mathcal{L}_{pg} encourages the model to increase the contribution weights for agent-dimension pairs that yield a high positive advantage. This loss is computed by summing the log-probability of the weights modulated by their respective advantages:

$$\mathcal{L}_{\text{pg}} = -\mathbb{E} \left[\sum_{i=1}^N \sum_{k=1}^C \log(W_{i,k}) \cdot A_{i,k} \right], \quad (8)$$

where $A_{i,k}$ is the k -th component of \mathbf{A}_i .

3.3.3. SHAPLEY REGULARIZATION LOSS

While the policy-gradient objective \mathcal{L}_{pg} enables the model to adapt to empirical utility, it is inherently susceptible to high-variance and stochastic reward fluctuations due to sample-wise advantage estimation. To mitigate this instability, we introduce a regularization term $\mathcal{L}_{\text{shap}}$ grounded in Shapley value (Shapley, 1953; Beechey et al., 2023).

We define the target as the C -dimensional Shapley matrix $\Phi \in \mathbb{R}^{N \times C}$, where $\Phi_{i,k}$ quantifies the contribution of agent i to decision dimension k . Specifically, $\Phi_{i,k}$ is approximated via Monte Carlo estimation of the Shapley value over M random coalitions $S \subseteq \mathcal{N} \setminus \{i\}$:

$$\Phi_{i,k} \approx \frac{1}{M} \sum_{m=1}^M \left[\mathcal{L}_k^{\text{BCE}}(S_m, \mathbf{y}) - \mathcal{L}_k^{\text{BCE}}(S_m \cup \{i\}, \mathbf{y}) \right]_+. \quad (9)$$

Here, $\mathcal{L}_k^{\text{BCE}}(S, \mathbf{y})$ denotes the BCE loss for output dimension k evaluated using only the agents in coalition S , and $\mathcal{L}_k^{\text{BCE}}(S \cup \{i\}, \mathbf{y})$ is the corresponding loss after adding agent i . The loss difference therefore captures the marginal utility of agent i relative to the baseline coalition S . This construction enables fine-grained credit assignment by explicitly measuring how each agent improves task performance across output dimensions. The resulting Shapley matrix Φ is normalized such that $\sum_{i,k} \Phi_{i,k} = 1$.

Then, the Shapley regularization loss is defined as the Kullback–Leibler divergence between \mathbf{W} and Φ , computed by summing over all components:

$$\mathcal{L}_{\text{shap}} = \mathbb{E} \left[\sum_{i=1}^N \sum_{k=1}^C W_{i,k} \log \left(\frac{W_{i,k}}{\Phi_{i,k}} \right) \right]. \quad (10)$$

This term regularizes \mathbf{W} by pulling it towards the estimated contribution Φ , thereby enforcing consistency between learned weights and cooperative game-theoretic credit assignment, as illustrated in Figure 2(c). To improve distributional stability during training, we maintain an exponential moving average (EMA) of the Shapley matrix. More detailed derivation of the Shapley approximation scheme, along with a formal comparison to the advantage vector \mathbf{A} , is provided in Section A.2.

4. Experimental Results

4.1. Datasets

To evaluate the efficacy of the proposed framework within oncological decision-making settings, we conduct experiments across two distinct data sources. 1) HCC Tumorboard, a curated real-world clinical tumor board dataset, and 2) MTBBench, a public molecular tumor board benchmark (Vasilev et al., 2025). Further details on multimodal data variables and partitioning information are provided in Section A.1.

4.2. Implementation Details

We implement CoMMA using LangGraph (Chase, 2022) with Llama3.1-70B-Instruct (Grattafiori et al., 2024) as the backbone model for all experiments. We train separate model for each dataset. On the HCC Tumorboard dataset,

Table 2. Comparison on Tumor Treatment Recommendation / Progression / Recurrence Prediction Performance.

Methods	Agent	HCC Tumorboard [†]				MTBBench			
		Treatment Recommendation		Progression		Recurrence			
		AUC	Accuracy	AUC	Accuracy	AUC	Accuracy		
Locally Trainable Baselines									
XGBoost (Chen, 2016)	-	0.662 \pm 0.024	0.784 \pm 0.026	N/A [‡]	N/A	N/A	N/A		
LGBMClassifier (Ke et al., 2017)	-	0.683 \pm 0.027	0.795 \pm 0.015	N/A	N/A	N/A	N/A		
CatBoost (Prokhorenkova et al., 2018)	-	0.697 \pm 0.020	0.797 \pm 0.022	N/A	N/A	N/A	N/A		
Non-Trainable Online In-context Learning									
GPT 4.1 in-context learning	GPT 4.1	N/A [§]	0.784 \pm 0.007	N/A	0.485 \pm 0.113	N/A	0.425 \pm 0.086		
MDAgents - Basic (Kim et al., 2024)	GPT 4.1	N/A	0.744 \pm 0.017	N/A	0.636 \pm 0.074	N/A	0.515 \pm 0.113		
Non-Trainable Online Multi-Agents Baselines									
MDAgents - Intermediate (Kim et al., 2024)	GPT 4.1	N/A	0.717 \pm 0.018	N/A	0.576 \pm 0.042	N/A	0.485 \pm 0.043		
MDAgents - Advanced (Kim et al., 2024)	GPT 4.1	N/A	0.740 \pm 0.023	N/A	0.606 \pm 0.113	N/A	0.394 \pm 0.113		
MDAgents - Adaptive (Kim et al., 2024)	GPT 4.1	N/A	0.730 \pm 0.009	N/A	0.576 \pm 0.085	N/A	0.394 \pm 0.043		
MAC (Chen et al., 2025b)	GPT 4.1	N/A	0.735 \pm 0.028	N/A	0.455 \pm 0.074	N/A	0.424 \pm 0.113		
Locally Fine-tunable Multi-Agents									
CoMMA(Ours)	Llama3.1-70B-Instruct	0.750 \pm 0.008	0.831 \pm 0.010	0.595 \pm 0.061	0.697 \pm 0.086	0.656 \pm 0.204	0.818 \pm 0.074		

[†]The HCC tumor board dataset comprises multi-label annotations for eight treatment modalities; we report the mean performance across all categories.

[‡]Locally trainable baselines are restricted to pre-defined, structured data such as categorical inputs, thus processing the unstructured text in the MTBBench dataset is unavailable.

[§]Existing online in-context learning and multi-agent baselines provide narrative outputs that only support binary accuracy, thus AUC computation is not available.

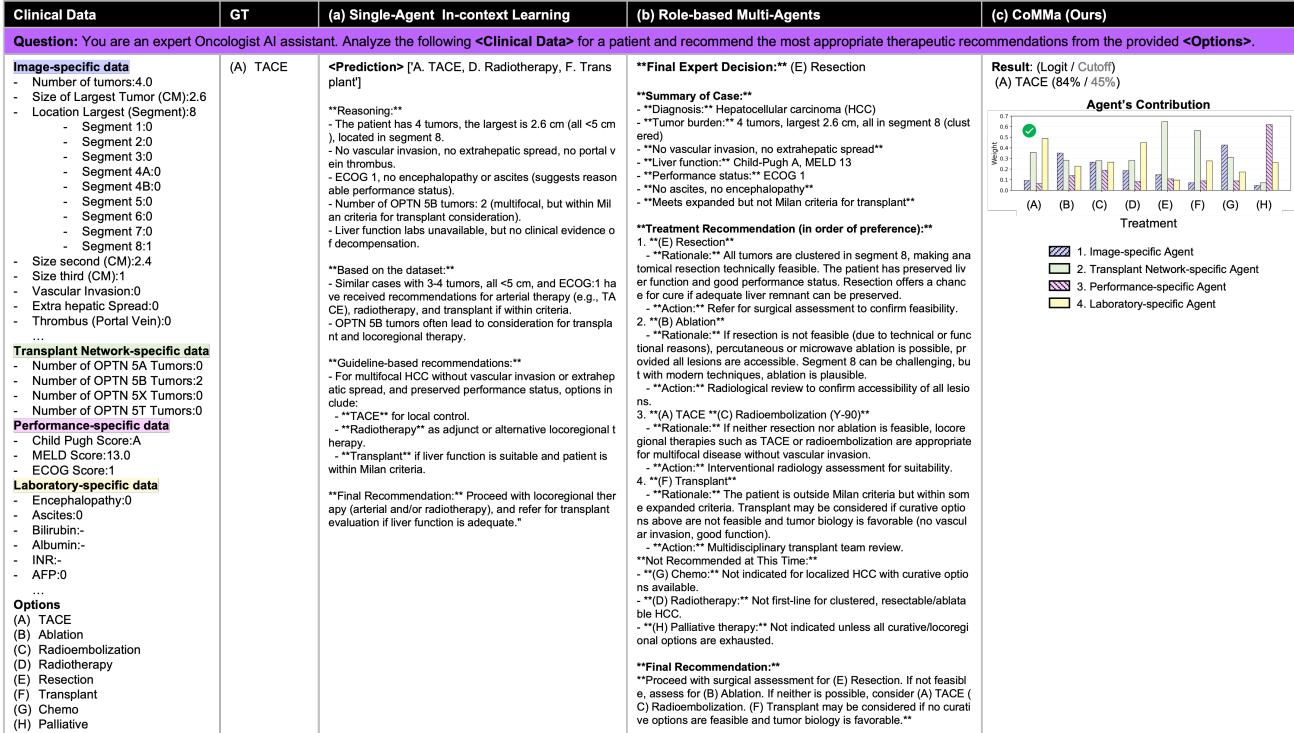


Figure 3. Agentic framework response comparison on HCC Tumorboard dataset. (a) Single-agent in-context learning (GPT-4.1), (b) Role-based multi-agent framework (MDAgents-Advanced), and (c) CoMMA. For the role-based multi-agent, intermediate discussions are omitted, and only the final consensus is visualized. For CoMMA, class-wise logits and cutoff thresholds are transformed into percentiles.

we train for 1000 epochs with a learning rate of 5×10^{-5} . On MTBBench dataset, we train for 30 epochs with a learning rate of 5×10^{-3} . In both settings, we use five agents, batch size of 4, and set the regularization weights to $\lambda_{pg} = 1$ and $\lambda_{shap} = 10$. We use two NVIDIA A100 80GB GPUs for training each model. In addition, we compare the computational complexity and inference cost of our model with those of the baseline methods in Section A.3.

4.3. Evaluation Methods

For evaluation, we report decision category-wise Area Under the ROC Curve (AUC) and Accuracy. AUC quantifies a model's discriminative ability to distinguish positive from negative outcomes. Accuracy is computed as,

$$\text{Accuracy} = \frac{1}{N} \sum_{i=1}^N \mathbb{I}(\hat{y}_{i,k} > t_k) = y_{i,k}. \quad (11)$$

where N denotes total number of evaluation dataset, t_k denotes the class-specific decision threshold determined on the training set, $\hat{y}_{i,k}$ is the predicted logit for decision category k , and $y_{i,k}$ is the corresponding ground-truth label. Due to the limited sample size of the multidisciplinary cohorts, we employ a robust evaluation framework with validation repeated across three random seeds. To mitigate sampling bias, label distributions are balanced during the training–evaluation splits. Model stability and performance are assessed by reporting the mean AUC and accuracy across all experimental runs.

4.4. Baseline Methods and Evaluation Methods

We evaluate our method against three categories of baseline approaches. For locally trainable baselines optimized for categorical and structured data, we employ XGBoost (Chen, 2016), LGBMClassifier (Ke et al., 2017), and CatBoost (Prokhorenkova et al., 2018). These locally trainable models operate exclusively on structured inputs, therefore, all clinical information is formatted as tabular features for these baselines, whereas our model consumes purely textual input. For non-trainable online in-context learning baselines, we use GPT-4.1, which also serves as the backbone for all non-trainable online multi-agent baselines. From MDAgents (Kim et al., 2024), we adopt the Basic setting, where a single agent performs in-context learning without explicit multi-agent interaction. For in-context learning, the entire training dataset with paired ground-truth annotations is provided as context. For non-trainable online multi-agent baselines, we include MDAgents (Kim et al., 2024) and MAC (Chen et al., 2025b), which simulates structured tumor board discussions. In MDAgents, the Intermediate setting induces discussions among five domain-specific specialists, while the Advanced setting organizes specialists into multiple tumor board teams and facilitates inter-team deliberation. In MAC, a single supervisor agent coordinates discussions among four doctor agents. We follow the formatted text prompts provided in the baseline models, with slight modifications to incorporate task-specific instructions. For all multi-agent baselines, GPT-4.1 is consistently used as the underlying agent model to ensure a fair comparison.

4.5. Results

4.5.1. ANALYSIS ON HCC TUMORBOARD

On the HCC Tumorboard treatment recommendation task, CoMMA achieves the strongest overall performance among all compared methods. As shown in Table 2, CoMMA attains an AUC of approximately 0.759 and an accuracy of tbd, substantially outperforming both locally trainable classical baselines and non-trainable LLM-based approaches. Compared to traditional machine learning models such as XGBoost, LightGBM, and CatBoost, CoMMA demon-

strates a clear advantage in capturing complex, heterogeneous clinical signals. Moreover, CoMMA also outperforms GPT-4.1 in-context learning and prior online multi-agent baselines, indicating that narrative discussion or retrieval-augmented prompting alone does not provide sufficiently reliable coordination for treatment recommendation. In contrast, CoMMA optimizes trainable multi-agent collaboration with a deterministic, contribution-aware credit assignment objective, explicitly rewarding agents based on marginal utility rather than stochastic dialogue heuristics. This yields more stable aggregation of evidence across decentralized partitions and translates into consistent improvements in recommendation quality, while providing agent-level attribution that is better aligned with clinical interpretability requirements. Detailed class-wise performance is provided in Section A.4.

We further qualitatively compare agentic framework responses in Figure 3. Single-agent and role-based multi-agent methods generate verbose textual rationales that are often misaligned with clinical context. In contrast, CoMMA provides quantitative attribution of agent contributions within standard decision logic, resulting in superior predictive performance. Although CoMMA does not produce fine-grained narratives, it yields compact, structured outputs that support clearer prediction. Additional response comparisons are provided in Section A.5.

4.5.2. ANALYSIS ON MTBBENCH

On MTBBench, we evaluate tumor progression and recurrence prediction, which require consolidating heterogeneous and longitudinal clinical evidence into a single outcome. As shown in Table 2, online LLM baselines and prior multi-agent discussion methods perform poorly and vary substantially across agent configurations, indicating fragile coordination and noisy evidence aggregation. In contrast, CoMMA achieves the best performance, attaining accuracies of 0.697 and 0.818 for progression and recurrence prediction, respectively. We attribute the gains to trainable multi-agent collaboration with deterministic, contribution-aware credit assignment, which leads to more stable and accurate outcome prediction under the challenging MTBBench setting.

4.5.3. ABLATION STUDY

We conduct ablation studies to disentangle the effects of CoMMA’s core components in Table 3. We first compare the single-agent stochastic narrative baseline (a) with deterministic embeddings (b), observing a 4% absolute improvement in accuracy. Beyond improved performance, deterministic embeddings enable gradient-based optimization and class-wise logit outputs, allowing AUC-based evaluation, which is infeasible with narrative generation alone. We then scale the number of agents from one (b) to five

Table 3. Ablation Study on CoMMA’s Core Components.

	# of Agents (N)	Deterministic Embedding	Data Decentralization	Agent-Decision Matrix	Contribution-Aware Multi-Agents	Agent	HCC Tumorboard [†]	
							Treatment Recommendation	
							AUC	Accuracy
CoMMA (Ours)	(a)	1				GPT 4.1	N/A [†]	0.784 ± 0.007
	(b)	1	✓			Llama3.1-70B-Instruct	0.714 ± 0.039	0.826 ± 0.014
	(c)	5	✓	✓		Llama3.1-70B-Instruct	0.730 ± 0.011	0.827 ± 0.009
	(d)	5	✓	✓	✓	Llama3.1-70B-Instruct	0.717 ± 0.008	0.826 ± 0.005
	(e)	5	✓	✓	✓	Llama3.1-70B-Instruct	0.750 ± 0.008	0.831 ± 0.010
Llama3.8B-Instruct								0.690 ± 0.006
Llama3.8B-Instruct								0.829 ± 0.014

[†]Online GPT 4.1 in-context learning provides narrative outputs that only support binary accuracy, thus AUC is not available.

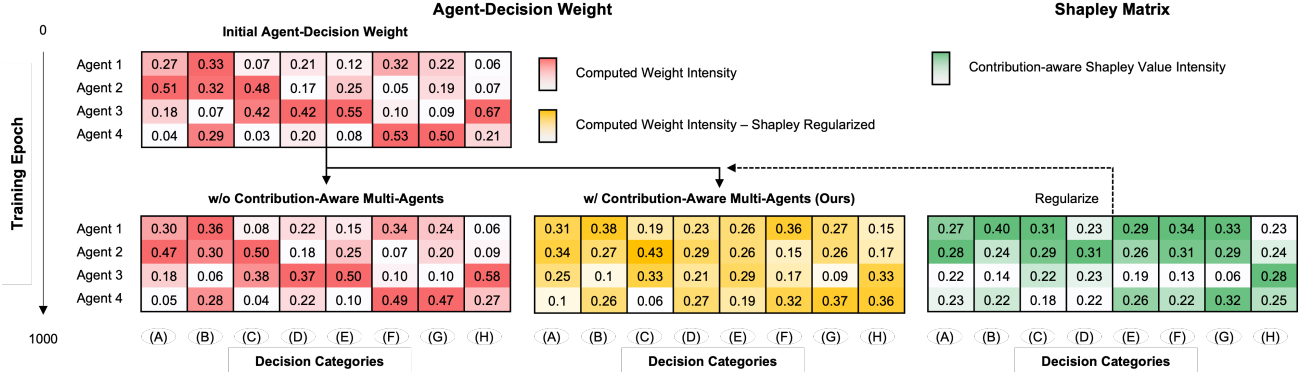


Figure 4. Visualization of agent-decision weights with and without the Contribution-Aware Multi-Agent module. With the module, weights converge toward the Shapley matrix over training, suppressing single-agent dominance. Columns are normalized to sum to 1.

data-decentralized agents without explicit coordination (c). This setting yields a notable improvement in AUC, while accuracy remains comparable. However, introducing a simple mixture via the agent-decision matrix (d) results in a slight performance decrease. These findings suggest that, even with decentralized agents, naive mixture weights are insufficient to fully exploit multi-agent reasoning and instead tend to overfit the training data. In contrast, CoMMA achieves a pronounced improvement in both AUC and accuracy relative to (d). This gain highlights the importance of contribution-aware learning over data-specified agents, as it explicitly models each agent’s marginal utility rather than treating agents as a weighted ensemble module. We further visualize the learned weight comparisons influenced by the Shapley matrix regularization in Figure 4. As training progresses, the initial agent-decision weights (\mathbf{W}) become closer to the contribution-aware Shapley matrix (Φ) than in the ablated setting. This indicates that disproportionate influence from any single agent is suppressed unless it contributes meaningfully to the objective. Finally, when replacing the agent backbone with a smaller LLM (Llama3-8B-Instruct) (e), performance decreases relative to the larger model. Notably, however, accuracy remains higher than that of the GPT-4.1 narrative baseline, suggesting that even smaller models, when embedded within a deterministic projection and contribution-aware framework, can outperform large-scale generative approaches, highlighting CoMMA’s

potential for efficient and scalable clinical deployment.

5. Conclusion, Limitations and Future Work

In this study, we proposed CoMMA, a contribution-aware medical multi-agent framework that replaces stochastic dialogue with deterministic specialization and structured credit assignment. Evaluations on oncology benchmarks demonstrate that CoMMA significantly improves predictive stability over centralized and narrative-based baselines. Moreover, CoMMA demonstrates that locally deployed architectures can achieve superior performance without relying on costly cloud-based inference or external data transfer. This marks a important step toward high-performance clinical AI in resource-constrained, privacy-sensitive settings.

Despite these strengths, our evaluation is currently constrained to specific oncology cohorts, reflecting the intrinsic scarcity and curation challenges of diverse real-world tumor board data. Furthermore, achieving granular reasoning remains challenging when processing highly clustered information across modalities. Future research will prioritize increasing data scale and disentangling data representations to enhance the resolution and minimize information entanglement. In addition, we will continue to address the limitations of the role-based multi-agents by further strengthening credit assignment principles to better capture the complex dynamics of oncology decision-making. Finally, the current

CoMMA instantiation is evaluated on tasks cast as discrete multiple-choice classification with clear ground-truth labels, which does not fully reflect the open-ended, often ambiguous nature of real-world multidisciplinary decision-making. Extending contribution-aware multi-agent modeling to settings involving free-form queries, partially observed or uncertain outcomes, and inherently ambiguous decision spaces represents an important direction for future research.

Impact Statement

Our framework introduces explicit game-theoretic attribution to quantify data contributions, mitigating risks associated with hallucinations and reasoning errors in clinical LLMs. By enabling a locally deployable multi-agent system, it supports privacy-preserving clinical AI without reliance on costly online inference. We believe this research direction promotes more equitable clinical AI applications.

References

Almansoori, M., Kumar, K., and Cholakkal, H. Medagentsim: Self-evolving Multi-agent Simulations for Realistic Clinical Interactions. In *International Conference on Medical Image Computing and Computer-Assisted Intervention*, pp. 362–372, 2025.

Beechey, D., Smith, T. M. S., and Şimşek, O. Explaining Reinforcement Learning with Shapley Values. In *International Conference on Machine Learning*, pp. 2003–2014, 2023.

Chase, H. Langchain, 2022. URL <https://github.com/langchain-ai/langchain>.

Chen, T. Xgboost: A Scalable Tree Boosting System. *Cornell University*, 2016.

Chen, X., Xiang, J., Lu, S., Liu, Y., He, M., and Shi, D. Evaluating Large Language Models and Agents in Healthcare: Key Challenges in Clinical Applications. *Intelligent Medicine*, 5(2):151–163, 2025a.

Chen, X., Yi, H., You, M., Liu, W., Wang, L., Li, H., Zhang, X., Guo, Y., Fan, L., Chen, G., et al. Enhancing Diagnostic Capability with Multi-agents Conversational Large Language Models. *NPJ digital medicine*, 8(1):159, 2025b.

Daye, D., Parker, R., Tripathi, S., Cox, M., Brito Obama, S., Valentin, L., Bridge, C. P., and Uppot, R. N. Cascade: Context-aware Data-driven AI for Streamlined Multidisciplinary Tumor Board Recommendations in Oncology. *Cancers*, 16(11):1975, 2024.

Dutang, C., Albrecher, H., and Loisel, S. Competition Among Non-life Insurers under Solvency Constraints: A Game-theoretic Approach. *European Journal of Operational Research*, 231(3):702–711, 2013.

Fallahpour, A., Ma, J., Munim, A., Lyu, H., and Wang, B. Medrax: Medical Reasoning Agent for Chest X-ray. In *International Conference on Machine Learning*, pp. 15661–15676, 2025.

Fan, Z., Wei, L., Tang, J., Chen, W., Siyuan, W., Wei, Z., and Huang, F. AI Hospital: Benchmarking Large Language Models in a Multi-agent Medical Interaction Simulator. In *International Conference on Computational Linguistics*, pp. 10183–10213, 2025.

Ferber, D., El Nahhas, O. S., Wölflein, G., Wiest, I. C., Clusmann, J., Leßmann, M.-E., Foersch, S., Lammert, J., Tschochohei, M., Jäger, D., et al. Development and validation of an Autonomous Artificial Intelligence Agent for Clinical Decision-making in Oncology. *Nature cancer*, pp. 1–13, 2025.

Grattafiori, A., Dubey, A., Jauhri, A., Pandey, A., Kadian, A., Al-Dahle, A., Letman, A., Mathur, A., Schelten, A., Vaughan, A., et al. The Llama 3 Herd of Models. *arXiv preprint arXiv:2407.21783*, 2024.

Han, X., Gao, X., Qu, X., and Yu, Z. Multi-Agent Medical Decision Consensus Matrix System: An Intelligent Collaborative Framework for Oncology MDT Consultations. *arXiv preprint arXiv:2512.14321*, 2025.

Ho, E., Rajagopalan, A., Skvortsov, A., Arulampalam, S., and Piraveenan, M. Game Theory in Defence Applications: A Review. *Sensors*, 22(3):1032, 2022.

Johri, S., Jeong, J., Tran, B. A., Schlessinger, D. I., Wongvibulsin, S., Barnes, L. A., Zhou, H.-Y., Cai, Z. R., Van Allen, E. M., Kim, D., et al. An Evaluation Framework for Clinical Use of Large Language Models in Patient Interaction Tasks. *Nature medicine*, 31(1):77–86, 2025.

Ke, G., Meng, Q., Finley, T., Wang, T., Chen, W., Ma, W., Ye, Q., and Liu, T.-Y. Lightgbm: A Highly Efficient Gradient Boosting Decision Tree. *Advances in Neural Information Processing Systems*, pp. 3147, 2017.

Kim, Y., Park, C., Jeong, H., Chan, Y. S., Xu, X., McDuff, D., Lee, H., Ghassemi, M., Breazeal, C., and Park, H. W. MDagents: An Adaptive Collaboration of LLMs for Medical Decision-making. *Advances in Neural Information Processing Systems*, pp. 79410–79452, 2024.

Lanctot, M., Zambaldi, V., Gruslys, A., Lazaridou, A., Tuyls, K., Pérolat, J., Silver, D., and Graepel, T. A Unified Game-theoretic Approach to Multiagent Reinforcement Learning. In *Advances in Neural Information Processing Systems*, pp. 4193–4206, 2017.

Lau, C. W., Catchpole, D., Simoff, S., Zhang, D., and Nguyen, Q. V. A Game-theoretical Approach to Clinical Decision Making with Immersive Visualisation. *Applied Sciences*, 13(18):10178, 2023.

Mendonça, F. V., Catalao-Lopes, M., Marinho, R. T., and Figueira, J. R. Improving Medical Decision-making with a Management Science Game Theory Approach to Liver Transplantation. *Omega*, 94:102050, 2020.

Parsons, S. and Wooldridge, M. Game Theory and Decision Theory in Multi-agent Systems. *Autonomous Agents and Multi-Agent Systems*, 5(3):243–254, 2002.

Patkar, V., Acosta, D., Davidson, T., Jones, A., Fox, J., and Keshtgar, M. Cancer Multidisciplinary Team Meetings: Evidence, Challenges, and the Role of Clinical Decision Support Technology. *International Journal of Breast Cancer*, 2011(1):831605, 2011.

Prokhorenkova, L., Gusev, G., Vorobev, A., Dorogush, A. V., and Gulin, A. Catboost: Unbiased Boosting with Categorical Features. In *Advances in Neural Information Processing Systems*, pp. 6638–6648, 2018.

Shapley, L. A Value For n-Person Games'. *Contributions to the Theory of Games*, (28):307, 1953.

Tang, X., Zou, A., Zhang, Z., Li, Z., Zhao, Y., Zhang, X., Cohan, A., and Gerstein, M. Medagents: Large Language Models as Collaborators for Zero-shot Medical Reasoning. In *Findings of the Association for Computational Linguistics*, pp. 599–621, 2024.

Tang, X., Shao, D., Sohn, J., Chen, J., Zhang, J., Xiang, J., Wu, F., Zhao, Y., Wu, C., Shi, W., et al. Medagentsbench: Benchmarking Thinking Models and Agent Frameworks for Complex Medical Reasoning. *arXiv preprint arXiv:2503.07459*, 2025.

Taylor, C., Munro, A. J., Glynne-Jones, R., Griffith, C., Trevatt, P., Richards, M., and Ramirez, A. J. Multidisciplinary Team Working in Cancer: What is the Evidence? *British Medical Journal*, 340:743–745, 2010.

Vasilev, K., Misrahi, A., Jain, E., Cheng, P. F., Liakopoulos, P., Michielin, O., Moor, M., and Bunne, C. MTBBench: A Multimodal Sequential Clinical Decision-Making Benchmark in Oncology. *Advances in Neural Information Processing Systems Datasets and Benchmarks Track*, 2025.

Von Neumann, J. and Morgenstern, O. Theory of Games and Economic Behavior: 60th Anniversary Commemorative Edition. In *Theory of Games and Economic Behavior*. Princeton University Press, 2007.

Wang, Z., Wu, J., Cai, L., Low, C. H., Yang, X., Li, Q., and Jin, Y. MedAgent-Pro: Towards Evidence-Based Multi-Modal Medical Diagnosis via Reasoning Agentic Workflow. *arXiv preprint arXiv:2503.18968*, 2025.

Zhang, W., Qiao, M., Zang, C., Niederer, S., Matthews, P. M., Bai, W., and Kainz, B. Multi-Agent Reasoning for Cardiovascular Imaging Phenotype Analysis. In *International Conference on Medical Image Computing and Computer-Assisted Intervention*, pp. 429–439, 2025.

Zhou, Y., Song, L., and Shen, J. MAM: Modular Multi-Agent Framework for Multi-Modal Medical Diagnosis via Role-Specialized Collaboration. *arXiv preprint arXiv:2506.19835*, 2025.

Zou, J. and Topol, E. J. The Rise of Agentic AI Teammates in Medicine. *The Lancet*, 405(10477):457, 2025.

A. Appendix

A.1. Dataset Details.

A.1.1. HCC TUMORBOARD

HCC Tumorboard dataset comprises a total of 116 patients diagnosed with primary Hepatocellular Carcinoma (HCC) at Massachusetts General Hospital (MGH), Boston, USA (Daye et al., 2024). The data collected for this study has been ethically approved by the IRB of the Department of Radiology at MGH (IRB #2022P001512). The study cohort includes patients who had a confirmed diagnosis of hepatocellular carcinoma (HCC) with no other concurrent malignancies, were reviewed by the multidisciplinary tumor board at MGH between August 2017 and August 2019, and were 18 years of age or older. Each case was reviewed by a multidisciplinary tumor board to establish the consensus treatment recommendation, serving as the ground truth labels. We filter out cases that lack recommendations in all categories. For the HCC dataset, we adopt a 75 / 25 % train-test split. The ground truth label is defined by 8 discrete treatment options: (A) Transcatheter Arterial Chemoembolization (TACE), (B) Ablation, primarily Microwave Ablation (MWA), (C) Radioembolization, also termed Selective Internal Radiation Therapy (SIRT), (D) Radiotherapy, (E) Surgical resection, (F) Liver transplant, (G) Chemotherapy, and (J) Palliative. The clinical data for each instance comprises 24 multimodal variables represented in a textual format, which extracted from the longitudinal clinical records and Magnetic Resonance Imaging (MRI) scans. We further provide an exemplar case illustrating the formation of the HCC Tumor Board dataset in Table 4.

Table 4. HCC Tumorboard Data Formation.

Decentralized Data					Global Data
	x_1 MRI imaging features	x_2 OPTN [†] information	x_3 Performance score	x_4 Laboratory data	x_{global} Concatenated Input
Context example	Number of tumors: 4.0 Size of largest tumor (cm): 2.6 Location largest (segment): 8 Vascular invasion: 0 Extrahepatic spread: 0 Thrombus (portal vein): 0 ⋮	Number of OPTN 5A tumors: 0 Number of OPTN 5B tumors: 2 Number of OPTN 5X tumors: 0 Number of OPTN 5T tumors: 0	Child-Pugh score: A ECOG [‡] score: 1 MELD [§] score: 13.0	Encephalopathy: 0 Ascites: 0 Bilirubin: 0.6 Albumin: 4.8 INR: 1.1 AFP: 5.0 ⋮	$[x_1, x_2, \dots, x_{N-1}]$

[†]OPTN: Organ Procurement & Transplantation Network, [‡]ECOG: Eastern Cooperative Oncology Group Performance, [§]MELD: Model for End-stage Liver Disease

A.1.2. MTBBENCH

MTBBench dataset (Vasilev et al., 2025) is an agentic benchmark designed to evaluate molecular tumor board-style reasoning that requires integrating multimodal evidence and longitudinal patient context. It contains 66 patient cases and 573 expert-validated question-answer pairs across two tracks. The multimodal track includes 26 head and neck cancer cases, with roughly 40 modality-specific files per patient, such as H and E slides, IHC images, and hematology reports, resulting in 390 questions. The longitudinal track includes 40 cases with about five structured files per patient and 183 questions focused on time-dependent outcomes, including recurrence and progression. In our experiments, we focus on prognosis prediction tasks for tumor recurrence and progression. Each case consists of a paired question and a binary classification label. For the MTBBench dataset, we adopt a 80 / 20 % train-test split. We further provide an exemplar case illustrating the formation of the MTBBench dataset in Table 5.

Table 5. MTBBench Data Formation.

Decentralized Data					Global Data
	x_1 Specimen metadata	x_2 Somatic mutations	x_3 Copy number alterations	x_4 Structural variants	x_{global} A timeline of clinical events
Context example	Colon Adenocarcinoma Primary (Sigmoid Colon) Tumor Purity: 20.0% MSI Type: Stable ⋮	TP53 p.C242F FANCA p.V750M CDK12 p.S238* ⋮	ERBB2 gain (Value: 2.0)% CDK12 gain (Value: 2.0) ⋮	CTNNB1 Splice Site deletion (c.18_242-37del) ⋮	Age 53: Stage IV Diagnosis → Surgery → Chemo (Oxaliplatin, Fluorouracil) ⋮

A.2. Detailed Shapley Approximation.

We redefine the Shapley matrix approximation in Equation (9) for a more detailed explanation as follows:

$$\Phi_{i,k} \approx \frac{1}{M} \sum_{m=1}^M \left[\mathcal{L}_k^{BCE}(S_m, \mathbf{y}) - \mathcal{L}_k^{BCE}(S_m \cup \{i\}, \mathbf{y}) \right]_+. \quad (12)$$

A.2.1. SHAPLEY VALUE APPROXIMATION STRATEGY

Exact computation of the Shapley value is computationally expensive, especially as the number of agents N increases. To achieve a tractable yet accurate approximation, we employ Monte Carlo sampling over $M = 2^{N/2}$ randomly sampled marginal contributions, where N denotes the total number of agents. This strategy substantially reduces computational complexity while preserving the statistical fidelity of the Shapley estimation. Furthermore, although the classical Shapley value admits both positive and negative contributions, we apply a rectified linear unit (ReLU) operator $[\cdot]_+$ to enforce non-negativity. This modification ensures that the resulting Shapley estimates form a valid target distribution for the KL divergence regularization in Equation (10), and that agents are credited exclusively for reducing the task loss.

A.2.2. COMPARISON TO ADVANTAGE VECTOR

Unlike the advantage vector \mathbf{A}_i , as introduced in Section 3.3.1, which only considers the marginal impact of removing agent i from the full coalitions \mathcal{N} , Shapley value defined in Equation (12) evaluates the contribution of agent i across a diverse set of sub-coalitions $S \subseteq \mathcal{N} \setminus \{i\}$ of varying cardinalities. Consequently, the resulting Shapley matrix Φ captures an expected marginal contribution that explicitly accounts for inter-agent interactions and dependencies, rather than being dominated by sample-specific or coalition-dependent fluctuations.

A.3. Comparison on Computational Cost.

We compare computational complexity and cost across trainable baselines, single-agent in-context learning, role-based multi-agent systems, and our locally fine-tunable multi-agent approach in Table 6. Latency and inference token usage are averaged over 30 samples from the HCC Tumorboard dataset. Our results show that CoMMA is a cost-effective method, achieving lower latency under a free-inference setting while delivering superior performance.

Table 6. Computational Complexity and cost Comparison on HCC Tumorboard Dataset.

Methods	Trainable Baselines	Single-Agent In-context Learning	Role-based Multi-Agents	Locally Fine-tunable Multi-Agents
	CatBoost	GPT 4.1	MDAgents - Advanced	CoMMA
Computational Complexity	0.048 MFLOPs	Unreleased	Unreleased	280 TFLOPs
Total Trainable Parameters	0.512 M	None	None	16.8 M
Latency (per input)	0.116 ms	4.2 s	79.2 s	1.1 s
Inference Tokens (chargeable)	None	20,878	23,254	None

A.4. Detailed Class-wise Performance Comparison on HCC Treatments.

A.5. Additional Response Comparison.

A.5.1. HCC TUMORBOARD

We further provide agentic framework response comparison on HCC Tumorboard dataset in Figure 5 and Figure 6. Whereas single-agent in-context learning and role-based multi-agent methods often yield verbose yet clinically inconsistent rationales, CoMMA provides quantitative attribution of agent contributions within a structured decision framework, resulting in superior predictive performance.

A.5.2. MTBBENCH

We provide a comparison of agentic framework responses on the MTBbench dataset. Specifically, we present a representative sample from each tumor progression tasks in Figure 7 and tumor recurrence prediction tasks in Figure 8. We observe that despite the extensive reasoning produced by both single-agent in-context learning and role-based multi-agent frameworks, their predictive accuracy remains significantly inferior to our proposed method.

Table 7. Comparison on HCC Tumorboard with Treatment Recommendation Performance.

Methods	Agent	Metric	HCC Treatments [†]								
			Average	(A)	(B)	(C)	(D)	(E)	(F)	(G)	(H)
Trainable Baselines											
XGBoost (Chen, 2016)	-	AUC	0.667 ± 0.009	0.649	0.674	0.512	0.533	0.796	0.706	0.652	0.817
		Accuracy	0.784 ± 0.026	0.696	0.697	0.805	0.752	0.817	0.772	0.805	0.929
LGBMClassifier (Ke et al., 2017)	-	AUC	0.683 ± 0.027	0.589	0.672	0.544	0.535	0.795	0.710	0.708	0.909
		Accuracy	0.795 ± 0.015	0.659	0.686	0.884	0.731	0.884	0.670	0.916	0.929
CatBoost (Prokhorenkova et al., 2018)	-	AUC	0.697 ± 0.020	0.586	0.751	0.675	0.596	0.812	0.671	0.717	0.768
		Accuracy	0.797 ± 0.022	0.672	0.697	0.850	0.765	0.908	0.637	0.916	0.929
Non-Trainable Online In-context Learning[‡]											
GPT 4.1	GPT 4.1	Accuracy	0.784 ± 0.007	0.722	0.711	0.832	0.722	0.821	0.589	0.943	0.931
MDAgents - Basic (Kim et al., 2024)	GPT 4.1	Accuracy	0.744 ± 0.017	0.666	0.733	0.711	0.767	0.667	0.645	0.922	0.845
Non-Trainable Online Multi-Agents Baselines											
MDAgents - Intermediate (Kim et al., 2024)	GPT 4.1	Accuracy	0.717 ± 0.018	0.645	0.632	0.767	0.722	0.611	0.611	0.878	0.867
MDAgents - Advanced (Kim et al., 2024)	GPT 4.1	Accuracy	0.740 ± 0.023	0.733	0.667	0.745	0.744	0.600	0.678	0.911	0.844
MDAgents - Adaptive (Kim et al., 2024)	GPT 4.1	Accuracy	0.730 ± 0.009	0.689	0.645	0.722	0.744	0.644	0.678	0.855	0.866
MAC (Chen et al., 2025b)	GPT 4.1	Accuracy	0.735 ± 0.028	0.689	0.722	0.733	0.744	0.633	0.600	0.900	0.856
Locally Fine-tunable Multi-Agents											
CoMMA(Ours)	Llama3.1-70B-Instruct	AUC	0.750 ± 0.008	0.600	0.782	0.582	0.585	0.929	0.668	0.901	0.947
		Accuracy	0.831 ± 0.010	0.733	0.733	0.883	0.767	0.934	0.700	0.934	0.967

[†]HCC Treatments Options: (A) TACE, (B) Ablation, (C) Radioembolization, (D) Radiotherapy, (E) Surgical resection, (F) Transplant, (G) Chemotherapy, (H) Palliative.

[‡]Non-trainable online frameworks provide narrative outputs that only support binary accuracy, thus AUC calculation is not available.

Clinical Data	GT	(a) Single-Agent In-context Learning	(b) Role-based Multi-Agents	(c) CoMMA (Ours)
Question: You are an expert Oncologist AI assistant. Analyze the following <Clinical Data> for a patient and recommend the most appropriate therapeutic recommendations from the provided <Options>.				
Image-specific data <ul style="list-style-type: none"> Number of tumors:1 Size of Largest Tumor (CM):2.0 Location Largest (Segment):8 <ul style="list-style-type: none"> Segment 1:0 Segment 2:0 Segment 3:0 Segment 4A:0 Segment 4B:0 Segment 5:0 Segment 6:0 Segment 7:0 Segment 8:1 Size second (CM):- Size third (CM):- Vascular Invasion:0 Extra hepatic Spread:0 Thrombus (Portal Vein):0 ... Transplant Network-specific data <ul style="list-style-type: none"> Number of OPTN 5A Tumors:0 Number of OPTN 5B Tumors:0 Number of OPTN 5X Tumors:0 Number of OPTN 5T Tumors:0 Performance-specific data <ul style="list-style-type: none"> Child Pugh Score:- MELD Score:- ECOG Score: 0 Laboratory-specific data <ul style="list-style-type: none"> Encephalopathy:0 Ascites:0 Bilirubin:0.3 Albumin:4.0 INR:1.1 AFP:2.2 ... Options <ul style="list-style-type: none"> (A) TACE (B) Ablation (C) Radioembolization (D) Radiotherapy (E) Resection (F) Transplant (G) Chemo (H) Palliative 	(E) Resection <Prediction> [(B) Ablation, (E) Resection] **Reasoning:** <ul style="list-style-type: none"> The patient has a solitary HCC (Number of tumors: 1), size 2.0 cm, located in segment 8. No vascular invasion, no extrahepatic spread, no portal vein thrombus. Excellent performance status (ECOG 0), no encephalopathy, no ascites. Liver function is well preserved (Bilirubin 0.3, Albumin 4.0, INR 1.1). AFP is low (2.2). **In-context learning from dataset:** <ul style="list-style-type: none"> Cases 83 and 11 have nearly identical features (solitary 2.0 cm tumor, segment 8, no invasion, preserved liver function, ECOG 0-1), both recommended for ablation and/or resection. Current guidelines (AASLD, EASL) recommend ablation or resection for solitary tumors <3 cm, good performance status, and well-preserved liver function. **Summary:** Both percutaneous ablation and surgical resection are appropriate and potentially curative options. The choice depends on technical feasibility, patient preference, and comorbidity.	**Case Summary:** <ul style="list-style-type: none"> Number of tumors: 1 Size of largest tumor: 2.0 cm Location: Segment 8 No vascular invasion, extrahepatic spread, or portal vein thrombus Performance status (ECOG): 0 (fully active) No ascites or encephalopathy Liver function: Bilirubin 0.3, Albumin 4.0, INR 1.1 (all normal) AFP: 2.2 (not elevated) Child-Pugh and MELD scores not provided, but clinical and lab data suggest well-compensated liver function (likely Child-Pugh A) No evidence of advanced disease or poor functional status **Interpretation:** This patient has a single, small hepatocellular carcinoma (HCC) in segment 8, with preserved liver function and excellent performance status. There is no evidence of vascular invasion, extrahepatic spread, or portal vein thrombus.	Result: (Logit / Cutoff) (E) Resection (66% / 79%) (B) Ablation (85% / 64%) Agent's Contribution Treatment: (A) (B) (C) (D) (E) (F) (G) (H) Legend: 1. Image-specific Agent, 2. Transplant Network-specific Agent, 3. Performance-specific Agent, 4. Laboratory-specific Agent	

Figure 5. Additional agentic framework response comparison on HCC Tumorboard dataset - #1. (a) Single-agent in-context learning (GPT-4.1), (b) Role-based multi-agent framework (MDAgents-Advanced), and (c) CoMMA. For the role-based multi-agent, intermediate discussions are omitted, and only the final consensus is visualized. For CoMMA, class-wise logits and cutoff thresholds are transformed into percentiles.

Clinical Data	GT	(a) Single-Agent In-context Learning	(b) Role-based Multi-Agents	(c) CoMMA (Ours)																																												
Question: You are an expert Oncologist AI assistant. Analyze the following <Clinical Data> for a patient and recommend the most appropriate therapeutic recommendations from the provided <Options>.																																																
Image-specific data <ul style="list-style-type: none"> Number of tumors:2.0 Size of Largest Tumor (CM):7.9 Location Largest (Segment):7.8 <ul style="list-style-type: none"> Segment 1:0 Segment 2:0 Segment 3:0 Segment 4A:0 Segment 4B:0 Segment 5:0 Segment 6:0 Segment 7:1 Segment 8:1 Size second (CM):1.2 Size third (CM):- Vascular Invasion:1 Extra hepatic Spread:1 Thrombus (Portal Vein):0 ... Transplant Network-specific data <ul style="list-style-type: none"> Number of OPTN 5A Tumors:1 Number of OPTN 5B Tumors:0 Number of OPTN 5X Tumors:0 Number of OPTN 5T Tumors:0 Performance-specific data <ul style="list-style-type: none"> Child Pugh Score:- MELD Score:- ECOG Score:3 Laboratory-specific data <ul style="list-style-type: none"> Encephalopathy:0 Ascites:0 Bilirubin:1.2 Albumin:2.9 INR:1.2 AFP:1.5 ... Options <ul style="list-style-type: none"> (A) TACE (B) Ablation (C) Radioembolization (D) Radiotherapy (E) Resection (F) Transplant (G) Chemo (H) Palliative 	(H) Palliative <Prediction> [H. Palliative] <Rationale> <ul style="list-style-type: none"> - Number of tumors: 2 (largest 7.9 cm, second 1.2 cm; segments 7, 8) - Vascular invasion: Present (1) - Extrahepatic spread: Present (1) - ECOG: 3 (poor performance status) - Liver function: Bilirubin 1.2, Albumin 2.9, INR 1.2 (mild-moderate dysfunction) - No significant ascites or encephalopathy - AFP very low (1.5) <In-context comparison & guideline basis:> <ul style="list-style-type: none"> - In the provided dataset, patients with extrahepatic spread and poor performance status (ECOG 2-3) are consistently assigned 'H. Palliative' care (see dataset row 10, 21, 32, 39, 76). - According to international guidelines (ASLD, EASL, BCLC), extrahepatic spread and poor functional status (ECOG u22652) indicate advanced HC C, where best supportive care or palliative systemic therapy is recommended. - Locoregional therapies (arterial, ablation, radioembolization, resection, transplant) are reserved for patients without vascular invasion/extrahepatic spread and better performance status. <Treatment options for this patient:> <ul style="list-style-type: none"> - Palliative care (H): Focus on symptom management, quality of life, and supportive measures. - Systemic therapy may be considered, but ECOG 3 performance status limits tolerance and benefit. <Summary:> Given the advanced disease (vascular invasion, extrahepatic spread) and poor performance status (ECOG 3), the most appropriate recommendation is palliative care.	<Final Decision: H - Palliative Care> <Rationale:> Based on the comprehensive MDT assessment and the clinical data provided: <ul style="list-style-type: none"> - Tumor Burden: Two liver tumors, largest 7.9 cm, with vascular invasion and extrahepatic spread. - Performance Status: ECOG 3 (significantly impaired, mostly bed/chair-bound). - Liver Function: Preserved synthetic function (bilirubin, albumin, INR normal), no ascites or encephalopathy. - Contraindications to Disease-Directed Therapies: - Curative options: (resection, transplant, ablation) are not feasible due to advanced disease (vascular invasion, extrahepatic spread) and poor performance status. - Local therapies: (arterial, radioembolization, radiotherapy) are contraindicated by extrahepatic spread and ECOG 3. - Systemic therapy: (chemo, targeted) is of limited benefit and likely poorly tolerated in ECOG 3 patients. - Goal of Care: Focus should be on symptom management, quality of life, and supportive measures. <Conclusion:> Therefore, the only appropriate recommendation is: (H) Palliative No disease-directed therapy is indicated. Palliative care should be initiated, with consideration for symptom control, psychosocial support, and advanced care planning.	Result: (Logit / Cutoff) (H) Palliative (32% / 28%) Agent's Contribution <table border="1"> <caption>Approximate data from 'Agent's Contribution' chart</caption> <thead> <tr> <th>Treatment</th> <th>1. Image-specific Agent</th> <th>2. Transplant Network-specific Agent</th> <th>3. Performance-specific Agent</th> <th>4. Laboratory-specific Agent</th> </tr> </thead> <tbody> <tr><td>(A)</td><td>0.05</td><td>0.65</td><td>0.05</td><td>0.05</td></tr> <tr><td>(B)</td><td>0.15</td><td>0.25</td><td>0.05</td><td>0.05</td></tr> <tr><td>(C)</td><td>0.25</td><td>0.20</td><td>0.05</td><td>0.05</td></tr> <tr><td>(D)</td><td>0.15</td><td>0.25</td><td>0.05</td><td>0.05</td></tr> <tr><td>(E)</td><td>0.05</td><td>0.60</td><td>0.05</td><td>0.05</td></tr> <tr><td>(F)</td><td>0.05</td><td>0.45</td><td>0.05</td><td>0.05</td></tr> <tr><td>(G)</td><td>0.35</td><td>0.15</td><td>0.05</td><td>0.05</td></tr> <tr><td>(H)</td><td>0.05</td><td>0.20</td><td>0.05</td><td>0.05</td></tr> </tbody> </table>	Treatment	1. Image-specific Agent	2. Transplant Network-specific Agent	3. Performance-specific Agent	4. Laboratory-specific Agent	(A)	0.05	0.65	0.05	0.05	(B)	0.15	0.25	0.05	0.05	(C)	0.25	0.20	0.05	0.05	(D)	0.15	0.25	0.05	0.05	(E)	0.05	0.60	0.05	0.05	(F)	0.05	0.45	0.05	0.05	(G)	0.35	0.15	0.05	0.05	(H)	0.05	0.20	0.05	0.05
Treatment	1. Image-specific Agent	2. Transplant Network-specific Agent	3. Performance-specific Agent	4. Laboratory-specific Agent																																												
(A)	0.05	0.65	0.05	0.05																																												
(B)	0.15	0.25	0.05	0.05																																												
(C)	0.25	0.20	0.05	0.05																																												
(D)	0.15	0.25	0.05	0.05																																												
(E)	0.05	0.60	0.05	0.05																																												
(F)	0.05	0.45	0.05	0.05																																												
(G)	0.35	0.15	0.05	0.05																																												
(H)	0.05	0.20	0.05	0.05																																												

Figure 6. Additional agentic framework response comparison on HCC Tumorboard dataset - #2.(a) Single-agent in-context learning (GPT-4.1), (b) Role-based multi-agent framework (MDAgents-Advanced), and (c) CoMMA. For the role-based multi-agent, intermediate discussions are omitted, and only the final consensus is visualized. For CoMMA, class-wise logits and cutoff thresholds are transformed into percentiles.

Clinical Data	GT	(a) Single-Agent In-context Learning	(b) Role-based Multi-Agents	(c) CoMMA (Ours)										
Question: Given that the patient is 70 years old, will the cancer progress in the next 12 months? Analyze the following <Clinical Data>. Answer in <Options>.														
Specimen metadata CANCER_TYPE: Colorectal Cancer SAMPLE_PIE: Primary SAMPLE_CLASS: Tumor METASTATIC_SITE: Not Applicable PRIMARY_SITE: Sigmoid Colon CANCER_TYPE_DETAILED: Colon Adenocarcinoma GENE_PANEL: IMPACT410 SAMPLE_COVERAGE: 1390 TUMOR_PURITY: 20.0 ONCOTREE_CODE: COAD ...	(B) No	<p><Prediction> B) No</p> <p>**Rationale:**</p> <ul style="list-style-type: none"> The patient's cancer is colon adenocarcinoma, localized (Stage 1-3), with no evidence of metastasis, and is microsatellite stable (MSS). Over the past 12 months (from age 69 to 70), there have been multiple CT scans (at ages 69.091 and 69.990) showing no cancer progression. Tumor markers (CEA) remained low and stable (from 0.9 to 3.1 ng/mL; both within the normal or mildly elevated range and with no trend indicating aggressive progression). The patient received appropriate adjuvant chemotherapy (capecitabine, leucovorin, fluorouracil), and there is no evidence of recurrence or residual disease on imaging. Performance status was ECOG 0 (fully active) throughout the year. Mutation profile (APC, TP53, PIK3CA, etc.) is common in colorectal cancer but, in the absence of high-risk molecular features (e.g., MSI-high, BRAF V600E, or clear evidence of aggressive molecular subtype), does not independently predict imminent progression within a year. No clinical, radiographic, or laboratory evidence indicates progression. <p>**Based on similar cases in the <Dataset> (see, e.g., patient with no recurrence or progression in past 12 months and stable imaging/labs, who were predicted as "No"), and in accordance with clinical guidelines, the likelihood of progression in the next 12 months is low.**</p> <p>**Final Answer:** <Prediction> B) No </p>	<p>**Answer: B) No**</p> <p>**Detailed MDT Review and Rationale:**</p> <p>### 1. **Clinical Context**</p> <ul style="list-style-type: none"> **Patient:** 69-year-old White female **Diagnosis:** Colon adenocarcinoma, ascending colon, localized (Stage 1-3) **Microsatellite status:** MSS (Microsatellite Stable) **Tumor Mutational Burden (TMB):** 7.8 mutations/Mb (intermediate, n of high) **Performance Status:** ECOG 0 (fully active) **CEA:** 0.9 ng/ml at diagnosis, 3.1 ng/ml at 1 year (both within normal limits) **Treatment:** Capecitabine, Leucovorin, Fluorouracil (standard adjuvant chemotherapy) **Imaging:** Serial CT scans at diagnosis and at 1 year show no evidence of cancer or progression** **Clinical status at 1 year:** No evidence of disease (NED) <p>### 2. **Molecular Profile**</p> <ul style="list-style-type: none"> **Key mutations:** APC, TP53, PIK3CA, B2M, CTCF, HIST1H3E, KDR, NSD1, KDM6A These are common in colorectal cancer, but none indicate high risk of rapid progression in the absence of residual disease. **Evidence of high-risk features:** No MSI-H, no high TMB, no actionable fusions or amplifications. <p>### 3. **Current Status**</p> <ul style="list-style-type: none"> **No evidence of disease on imaging at 1 year** **Normal tumor marker (CEA)** **No clinical symptoms or findings suggestive of recurrence or progression** **No evidence of metastatic disease at any time** <p>### 4. **Risk of Progression**</p> <ul style="list-style-type: none"> **Localized, resected colon cancer** with adjuvant chemotherapy and no evidence of disease at 1 year has a **low risk of progression in the next 12 months**. **MSS status** and **absence of high-risk molecular features** further support a favorable prognosis. **Serial imaging and tumor markers** are negative for recurrence. <p>### Conclusion**</p> <p>Based on the available clinical, pathological, molecular, and radiologic data, there is no evidence to suggest that this patient's colon cancer will progress in the next 12 months. The risk of recurrence or progression is low given the current status. Continued surveillance is recommended as per guidelines, but at this time, the answer is:**</p> <p>**B) No, the cancer will not progress in the next 12 months.**</p>	<p>Result: (Logit / Cutoff) (B) No (53% / 56%)</p> <p>Agent's Contribution</p> <table border="1"> <caption>Data for Agent's Contribution Bar Chart</caption> <thead> <tr> <th>Category</th> <th>Weight</th> </tr> </thead> <tbody> <tr> <td>1. Specimen metadata</td> <td>~0.1</td> </tr> <tr> <td>2. Somatic mutations</td> <td>~0.3</td> </tr> <tr> <td>3. Copy number alterations</td> <td>~0.5</td> </tr> <tr> <td>4. Structural variants</td> <td>~0.05</td> </tr> </tbody> </table>	Category	Weight	1. Specimen metadata	~0.1	2. Somatic mutations	~0.3	3. Copy number alterations	~0.5	4. Structural variants	~0.05
Category	Weight													
1. Specimen metadata	~0.1													
2. Somatic mutations	~0.3													
3. Copy number alterations	~0.5													
4. Structural variants	~0.05													

Figure 7. Additional agentic framework response comparison on MTBBench - tumor progress question. (a) Single-agent in-context learning (GPT-4.1), (b) Role-based multi-agent framework (MDAgents-Advanced), and (c) CoMMA. For the role-based multi-agent, intermediate discussions are omitted, and only the final consensus is visualized. For CoMMA, class-wise logits and cutoff thresholds are transformed into percentiles.

Clinical Data	GT	(a) Single-Agent In-context Learning	(b) Role-based Multi-Agents	(c) CoMMa (Ours)																																		
Question: Given that the patient is 54.5 years old, will the cancer have a recurrence in the next 12 months? Analyze the following <Clinical Data>. Answer in <Options> .																																						
Specimen metadata CANCER_TYPE: Colorectal Cancer SAMPLE_P: Primary SAMPLE_C: Tumor METASTATIC_SITE: Not Applicable PRIMARY_SITE: Sigmoid Colon CANCER_TYPE_DETAILED: Colon Adenocarcinoma GENE_PANEL: IMPACT410 SAMPLE_COVERAGE: 1390 TUMOR_PURITY: 20.0 ONCOTREE_CODE: COAD ... Somatic mutations ... Copy number alterations ... Structural variants ... Options (A) Yes (B) No	(A) Yes	<p><Prediction> (B) No</p> <p>Reasoning:</p> <ul style="list-style-type: none"> - The patient is a 53-year-old White female with a history of stage IV (distant metastatic, AJCC IV) colon adenocarcinoma of the sigmoid colon. - She underwent systemic chemotherapy (oxaliplatin, leucovorin, fluorouracil) and has had frequent imaging and CEA monitoring. - Imaging (CT and MR) and CEA labs from age 53.5 through 54.5 consistently show: <ul style="list-style-type: none"> - No evidence of cancer recurrence or progression (multiple CT scans state "cancer has NOT progressed" and "HAS CANCER: No"). - CEA levels are low and stable (all ≤ 22641.8 ng/ml). - ECOG performance status remains 0 or 1. - Most recent imaging at age 54.495 (close to present age 54.5) shows no progression or presence of cancer. - She is microsatellite stable (MSS) and has a moderate tumor mutation burden (TMB). - There is no documentation of cancer recurrence or progression in the last 12 months. - Open-source clinical guidelines indicate that, while stage IV colorectal cancer carries a high risk of recurrence, stable imaging and tumor markers over a full year suggest the risk of recurrence in the next 12 months is relatively low (2014 especially with ongoing surveillance and no current evidence of disease). <p>Therefore, based on the comprehensive clinical data and absence of progression or new lesions in the past year, the best-supported prediction is:</p> <p>B) No, the cancer will NOT have a recurrence in the next 12 months.</p>	<p>Answer: B) No</p> <p>**Rationale and Detailed Review:**</p> <p>### 1. **Clinical Context**</p> <ul style="list-style-type: none"> - **Patient:** 54.5-year-old White female, non-Hispanic - **Diagnosis:** Colon adenocarcinoma, sigmoid colon, AJCC Stage IV (distant disease) - **Treatment:** Received standard chemotherapy (Oxaliplatin, Leucovorin, Fluorouracil) - **Performance Status:** ECOG 0-1 throughout, indicating good functional status - **Tumor Markers:** CEA consistently low ($1.1 \leq 20131.8$ ng/ml), CA19-9 mildly elevated once (46 U/ml) - **Imaging:** Serial CT and MR scans show no evidence of cancer progression or recurrence* at multiple time points up to age 54.495. <p>### 2. **Molecular and Pathological Data**</p> <ul style="list-style-type: none"> - **MSI Status:** Microsatellite stable (MSS), MSI score 0.21 (low risk for hypermutated phenotype) - **Tumor Mutational Burden (TMB):** 3.9 mutations/Mb (low-intermediate, not predictive of high recurrence risk) - **Key Mutations:** <ul style="list-style-type: none"> - **TP53 (missense):** Common in colorectal cancer, but not specifically predictive of recurrence in isolation. - **FANCA (missense):** DNA repair gene, but not a strong driver of recurrence risk. - **CDK12 (nonsense):** Loss-of-function, may affect DNA repair, but not a high-risk marker for recurrence in MSS CRC. - **CTNNB1 (splice site):** Wnt pathway, but not a strong recurrence predictor in this context. - **Copy Number Alterations:** Mild gains (ERBB2, CDK12, RARA, SUZ12, PRKAR1A), but no high-level amplifications or deletions associated with aggressive behavior. - **No structural variants detected.** <p>### 3. **Clinical Course and Surveillance**</p> <ul style="list-style-type: none"> - No prior medications before MSK treatment.** - Serial imaging (CT/MR) at ages 53.544, 53.947, 54.101, and 54.495: All show no evidence of active cancer* or progression.** - CEA levels remain stable and low, which is reassuring.** - Performance status remains good (ECOG 0-1).** <p>### 4. **Risk of Recurrence**</p> <ul style="list-style-type: none"> - Stage IV disease* does carry a risk of recurrence, but in this patient: - No radiological evidence of disease* for over 12 months. - No biochemical evidence of recurrence* (CEA stable and low). - No high-risk molecular features* (MSS, low TMB, no aggressive driver mutations). - No clinical deterioration.** <p>### 5. **Summary Table**</p> <table border="1"> <thead> <tr> <th>Factor</th> <th>Finding</th> <th>Recurrence Risk</th> </tr> </thead> <tbody> <tr> <td>Imaging</td> <td>No evidence of disease</td> <td>Low</td> </tr> <tr> <td>Tumor markers</td> <td>CEA stable, low</td> <td>Low</td> </tr> <tr> <td>MSI status</td> <td>Stable (MSS)</td> <td>Low</td> </tr> <tr> <td>TMB</td> <td>Low-intermediate</td> <td>Low</td> </tr> <tr> <td>Key mutations</td> <td>No high-risk drivers</td> <td>Low</td> </tr> <tr> <td>Performance status</td> <td>ECOG 0-1</td> <td>Low</td> </tr> <tr> <td>Clinical course</td> <td>No progression, good response</td> <td>Low</td> </tr> </tbody> </table> <p>Conclusion: Based on the comprehensive review of clinical, pathological, molecular, and imaging data, the risk of recurrence in the next 12 months is low*. There is no current evidence of active disease* or progression, and all surveillance parameters are reassuring.</p> <p>Final Decision:</p> <p>B) No, the cancer is unlikely to recur in the next 12 months given the patient's current clinical, imaging, and molecular profile.**</p> <p>Recommendations:</p> <ul style="list-style-type: none"> - Continue regular surveillance (imaging, CEA) as per guidelines. - Monitor for new symptoms. - Maintain multidisciplinary follow-up. 	Factor	Finding	Recurrence Risk	Imaging	No evidence of disease	Low	Tumor markers	CEA stable, low	Low	MSI status	Stable (MSS)	Low	TMB	Low-intermediate	Low	Key mutations	No high-risk drivers	Low	Performance status	ECOG 0-1	Low	Clinical course	No progression, good response	Low	<p>Result: (Logit / Cutoff) (A) Yes (49% / 47%)</p> <p>Agent's Contribution</p> <table border="1"> <caption>Data for Agent's Contribution Bar Chart</caption> <thead> <tr> <th>Factor</th> <th>Weight</th> </tr> </thead> <tbody> <tr> <td>1. Specimen metadata</td> <td>~0.12</td> </tr> <tr> <td>2. Somatic mutations</td> <td>~0.28</td> </tr> <tr> <td>3. Copy number alterations</td> <td>~0.55</td> </tr> <tr> <td>4. Structural variants</td> <td>~0.05</td> </tr> </tbody> </table>	Factor	Weight	1. Specimen metadata	~0.12	2. Somatic mutations	~0.28	3. Copy number alterations	~0.55	4. Structural variants	~0.05
Factor	Finding	Recurrence Risk																																				
Imaging	No evidence of disease	Low																																				
Tumor markers	CEA stable, low	Low																																				
MSI status	Stable (MSS)	Low																																				
TMB	Low-intermediate	Low																																				
Key mutations	No high-risk drivers	Low																																				
Performance status	ECOG 0-1	Low																																				
Clinical course	No progression, good response	Low																																				
Factor	Weight																																					
1. Specimen metadata	~0.12																																					
2. Somatic mutations	~0.28																																					
3. Copy number alterations	~0.55																																					
4. Structural variants	~0.05																																					

Figure 8. Additional agentic framework response comparison on MTBBench - tumor recurrence question. (a) Single-agent in-context learning (GPT-4.1), (b) Role-based multi-agent framework (MDAgents-Advanced), and (c) CoMMa. For the role-based multi-agent, intermediate discussions are omitted, and only the final consensus is visualized. For CoMMa, class-wise logits and cutoff thresholds are transformed into percentiles.